

Evolution of the composition of the zirconium alloy surface layer under external thermal influence

© A.L. Maslov, N.N. Nazarenko

Institute of Strength Physics and Materials Science, Siberian Branch, Russian Academy of Sciences,
634055 Tomsk, Russia
e-mail: masloaleksey@rambler.ru

Received March 27, 2023

Revised October 24, 2023

Accepted October 24, 2023

A macromodel of the composition evolution in a cylindrical sample under short-term thermal influence is presented. The model takes into account cross effects and chemical reactions. Stresses and deformations are evaluated. The value of stresses depends on the initial composition, chemical reactions and cross effects. The problem is extended to a micromodel in which diffusion near the sample surface is investigated. The micromodel takes into account the grain structure of the sample material and the phenomenon of mass flux relaxation during diffusion. The influence of relaxation times on the rate of formation of chemical reaction products is investigated.

Keywords: diffusion, zirconium alloys, grain boundaries, mechanical stresses, strains.

DOI: 10.61011/JTF.2024.01.56905.59-23

Introduction

Zirconium alloys are used as the main structural materials of reactor core parts and fuel assemblies of nuclear power reactors [1,2]. Cladding tubes are the most critical items since the failure of the reactor fuel element cladding during operation results in emergency situations and is practically unacceptable. Fuel element cladding operate in very challenging conditions of exposure to temperature, radiation, corrosive environment and stresses. External surfaces of fuel element cladding tubes are exposed to the corrosive impact of a coolant with a temperature up to 380°C, and released corrosion products can result in a local overheating as they impair heat transfer. Corrosion resistance is one of the key requirements for reactor core materials.

Zirconium and its alloys react with water in a liquid state and in the water vapor state. Zirconium is oxidized in the result of such reactions, the remaining hydrogen diffuses into the metal, and can react with it itself. This process has a significant impact on the properties of zirconium alloys and the performance of products made from zirconium alloys.

Hydrogen in metals has an unusually high diffusion mobility and at low temperatures as well. However, the diffusion mobility of hydrogen notably increases with the increase of the temperature. The diffusion constant used to quantify the hydrogen and oxygen diffusion processes in metals exponentially increases with the temperature increase. Zr absorbs hydrogen when heated above 250°C and forms ZrH_x compound of variable composition and hydrogen is released from this compound when temperature exceeds 400°C.

Stresses, as well as the occurrence of temperature or stress gradients have a significant impact on the rate of hydrogen diffusion in metals in addition to temperature.

Hydrogen diffuses in the area of the lowest temperatures and the greatest tensile stresses, forming local (brittle) zones with an increased level of hydrogenation.

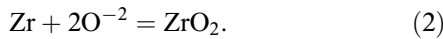
These materials, in addition to a low neutron absorption cross-section, should withstand a combination of challenging conditions of exposure to high doses of radiation, high temperatures, corrosion [3–6]. The application of various coatings and modification of the surfaces of products can be one of the possible ways to reduce the adverse effects of these factors [7]. It should be noted that the grain structure of the material, the difference of the properties of the intragrain region and the properties of the grain boundary region, etc. can have a significant impact on the diffusion process [8]. The latter is particularly true for materials with such a small grain size that a significant part of the material volume consists of grain boundaries (they are referred as nanocrystalline materials) [9]. Therefore, a particular interest is also posed by zirconium alloys formed by grains with size significantly less than 100 nm [10]. Therefore, it is important, in particular, to study the oxidation of zirconium alloys by oxygen in the temperature range of 600–1200 K, taking into account their granular structure. The authors of [11–14] investigated the properties and structural state of zirconium alloys in case of exposure to a pulsed electron beam (PEB) or a pulsed ion beam (PIB). They demonstrated that exposure to IPP and the formation of ZrO_2 can reduce the rate of hydrogen absorption and increase the product hydrogenation resistance.

This paper evaluates mechanical stresses in a cylindrical zirconium alloy sample subjected to external thermal pulses during diffusion into an oxygen and hydrogen alloy. A micromodel that takes into account the sample granular structure was used to study near surface diffusion. Only short duration, immediately related to the exposure are

considered in this paper. Long-term processes of important practical significance may be covered by other studies.

1. Problem formulation

Let's consider a tube made of zirconium alloy, which is a part of the core of the nuclear power reactor fuel assemblies (Fig. 1, *a*). It is exposed to corrosion during cool down. The additional zirconium hydride and zirconium oxide can be formed in the result of the following overall reactions owing to the diffusion of hydrogen and oxygen into the substrate (which originally consisted of a zirconium alloy):



There are 3 diffusants (Zr, H, O) and two chemical compounds concurrently in the system and their migration can be neglected.

The sample is represented as consisting of two regions such as grain-boundary and intragrain taking into account the granular structure of the material for studying the diffusion of hydrogen and oxygen in an alloy at the microlevel. The intragrain regions have the shape of identical rectangles located at the same distance from each other and separated by boundary regions (Fig. 1, *b*). These regions are characterized by different diffusion coefficients and rates of chemical reactions of diffusants with the sample material. Introducing the notation for concentrations shown in Table 1, we note the balance equations and kinetic equations in the following form

$$C_p \rho \frac{\partial T}{\partial t} = -\nabla \cdot \mathbf{J}_T + W, \quad (3)$$

$$\frac{\partial C_k}{\partial t} = -\nabla \cdot \mathbf{J}_k + r_k, \quad k = 1, 2 \quad (4)$$

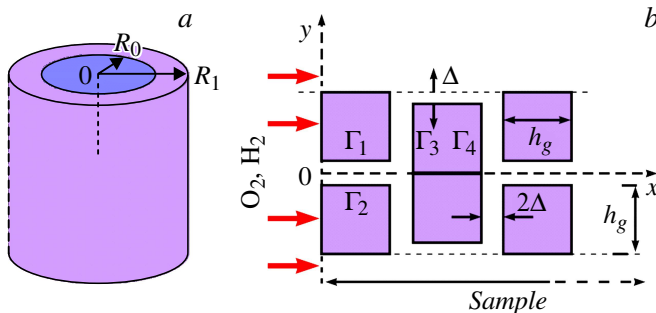


Figure 1. Illustration of the formulation of the problem at the macro level (*a*) and illustration of the formulation of the problem of grain boundary diffusion (*b*).

Table 1. Designations of concentrations

Substance	H ⁺	O ²⁻	Zr	ZrH ₂	ZrO ₂
Designation	C ₁	C ₂	C ₃	C ₄	C ₅

$$\rho \frac{C_i}{\partial t} = r_i, \quad i = 4, 5, \quad (5)$$

$$\sum_{j=1}^5 C_j = 1, \quad (6)$$

where T — temperature, [K]; ρ — density, [kg/m³]; C_p — isobaric heat capacity, [J/(kg·K)]; \mathbf{J}_q and \mathbf{J}_i — heat and mass fluxes, r_k — sources and drains of components in reactions; W — total chemical heat release.

Reaction rates depend on concentrations according to the law of the mass action, and on temperature according to the Arrhenius law:

$$\varphi_1 = k_1 C_3 C_1^2 \exp\left(-\frac{E_1}{RT}\right), \quad \varphi_2 = k_2 C_2^2 C_3 \exp\left(-\frac{E_2}{RT}\right). \quad (7)$$

In this case the mass sources and drains in chemical reactions will have the following form in accordance with (1), (2).

$$\begin{aligned} r_1 &= -\varphi_2, & r_2 &= -2\varphi_2, & r_3 &= -\varphi_1 - \varphi_2, \\ r_4 &= \varphi_1, & r_5 &= \varphi_2, \end{aligned} \quad (8)$$

and the total chemical heat release will have the following form

$$W = Q_1^\sigma \varphi_1 + Q_2^\sigma \varphi_2, \quad (9)$$

where k_i — pre-exponential factors, 1/s ($i = 1, 2$), E_i — activation energies ($i = 1, 2$), [J/mol]; Q_1^σ and Q_2^σ — heat of reactions. The heat and mass fluxes that take into account cross-phenomena, in accordance with [15] will be written as follows:

$$\mathbf{J}_1 = -\rho D_{11} \nabla C_1 - \rho D_{12} \nabla C_2 - C_1 D_{11} S_{T1} \rho \nabla T - t_1 \frac{\partial \mathbf{J}_1}{\partial t},$$

$$\mathbf{J}_2 = -\rho D_{21} \nabla C_1 - \rho D_{22} \nabla C_2 - C_2 D_{22} S_{T2} \rho \nabla T - t_2 \frac{\partial \mathbf{J}_2}{\partial t},$$

$$\mathbf{J}_q = -\lambda_T \nabla T - A_1 \nabla C_1 - A_2 \nabla C_2 - t_q \frac{\partial \mathbf{J}_q}{\partial t}. \quad (10)$$

where D_{ik} , A_1 , A_2 — transfer coefficients; $A_1 = D_{11} Q_1^* + D_{21} Q_2^*$, $A_2 = D_{12} Q_1^* + D_{22} Q_2^*$, including transfer heats $Q_k^* = \rho R T^2 S_{T k} f_{k k} m_k^{-1}$, $k = 1, 2$; m_k — molar masses of components, [kg/mol]; R — universal gas constant; t_q , t_k — relaxation times to the equilibrium state of heat and mass fluxes; $S_{T k}$ — Soret coefficients, related to the coefficients of thermodiffusion by the following relations:

$$S_{T1} = \frac{D_{T1}}{D_{11}}, \quad S_{T2} = \frac{D_{T2}}{D_{22}}. \quad (11)$$

We come to three second-order differential equations in both time and spatial variables by substituting (10) in (3) and (4):

$$\begin{aligned} t_q \rho C_\sigma \frac{\partial^2 T}{\partial t^2} + \rho C_\sigma \frac{\partial T}{\partial t} &= \nabla \cdot (\lambda_T \nabla T) \\ &+ \nabla \cdot (A_1 \nabla C_1) + \nabla \cdot (A_2 \nabla C_2) + t_q \frac{\partial W}{\partial t} + W, \end{aligned}$$

$$\begin{aligned}
t_1 \rho \frac{\partial^2 C_1}{\partial t^2} + \rho \frac{\partial C_1}{\partial t} &= \nabla \cdot (\rho D_{11} \nabla C_1) + \nabla \cdot (\rho D_{12} \nabla C_2) \\
&+ \nabla \cdot (C_1 D_{11} S_{T1} \rho \nabla T) + t_1 \rho \frac{\partial r_1}{\partial t} + \rho r_1, \\
t_2 \rho \frac{\partial^2 C_2}{\partial t^2} + \rho \frac{\partial C_2}{\partial t} &= \nabla \cdot (\rho D_{21} \nabla C_1) + \nabla \cdot (\rho D_{22} \nabla C_2) \\
&+ \nabla \cdot (C_2 D_{22} S_{T2} \rho \nabla T) + t_2 \rho \frac{\partial r_2}{\partial t} + \rho r_2.
\end{aligned} \tag{12}$$

We come to a one-dimensional problem in a cylindrical coordinate system assuming that the heat flux is uniformly distributed over the side surface of a cylindrical part, and its ends are thermally insulated:

$$\begin{aligned}
t_q \rho C_\sigma \frac{\partial^2 T}{\partial t^2} + \rho C_\sigma \frac{\partial T}{\partial t} &= \frac{1}{r} \frac{\partial}{\partial r} \\
&\times \left[r \lambda_T \frac{\partial T}{\partial r} + r A_1 \frac{\partial C_1}{\partial r} + r A_2 \frac{\partial C_2}{\partial r} \right] + t_q \frac{dW}{dt} + W, \\
t_1 \rho \frac{\partial^2 C_1}{\partial t^2} + \rho \frac{\partial C_1}{\partial t} &= \frac{1}{r} \frac{\partial}{\partial r} \\
&\times \left[r C_1 D_{11} S_{T1} \rho \frac{\partial T}{\partial r} + r \rho D_{11} \frac{\partial C_1}{\partial r} + r \rho D_{12} \frac{\partial C_2}{\partial r} \right] \\
&+ t_1 \rho \frac{\partial r_1}{\partial t} + \rho r_1, \\
t_2 \rho \frac{\partial^2 C_2}{\partial t^2} + \rho \frac{\partial C_2}{\partial t} &= \frac{1}{r} \frac{\partial}{\partial r} \\
&\times \left[r C_2 D_{22} S_{T2} \rho \frac{\partial T}{\partial r} + r \rho D_{21} \frac{\partial C_1}{\partial r} + r \rho D_{22} \frac{\partial C_2}{\partial r} \right] \\
&+ \rho t_2 \frac{\partial r_2}{\partial t} + \rho r_2.
\end{aligned} \tag{13}$$

$$t = 0: C_i = C_{i0}(r); \quad .i = 1 - 5; \quad T = T_0$$

$$r = R_0: \mathbf{J}_i = 0, \quad i = 1, 2, \quad \mathbf{J}_q = 0;$$

$$r = R_1: \mathbf{J}_i = 0, \quad i = 1, 2, \quad J_q = \begin{cases} q_0, & t < t_i, \\ 0, & t \geq t_i. \end{cases}$$

Let's consider the subproblem of diffusion at the microlevel in a rectangular coordinate system. Let the upper index at the concentration of the diffusant indicate its location: B — in the grain boundary region, G — in the intragrain region (Fig. 1, b). We will consider this subproblem in an isothermal approximation, neglecting cross-effects.

The diffusion equations for this case have the following form

$$\begin{aligned}
t_i^j \rho \frac{\partial^2 C_i^j}{\partial t^2} + \rho \frac{\partial C_i^j}{\partial t} \\
= \rho D_i^j \nabla \cdot (\nabla C_{i,B}) - t_i^j \rho \frac{\partial r_i^j}{\partial t} - \rho r_i^j,
\end{aligned}$$

$$i = 1, 2, \quad j = B, G. \tag{14}$$

In this case the diffusant fluxes have the following form in the intragrain and grain boundary regions

$$\mathbf{J}_i^j = -D_i^j \rho \nabla C_i^j - t_i^j \frac{\partial \mathbf{J}_i^j}{\partial t}, \quad i = 1, 2, \quad j = B, G. \tag{15}$$

The kinetic equations are similar to the equations from (13), with the difference that they take into account the difference of reaction rates in different areas:

$$\rho \frac{dC_i^j}{dt} = r_i^j, \quad i = 4, 5, \quad j = B, G. \tag{16}$$

The concentration of C_5^j can be found from the mass balance equation (6). There is no diffusant in the substrate at the initial moment of time, there are also no reaction products:

$$\begin{aligned}
t = 0: C_1^j = C_2^j = C_4^j = C_5^j = \frac{\partial C_1^j}{\partial t} = \frac{\partial C_2^j}{\partial t} = 0, \\
j = B, C.
\end{aligned}$$

Concentrations of diffusants are defined at the outer boundary

$$x = 0: C_1 = C_{01}, \quad C_2 = C_{02}. \tag{17}$$

Conditions of the fourth kind are fulfilled at all internal borders. For example, for $0 \leq x \leq h_g, y = \Delta$:

$$C_1^B = C_1^G, \quad \mathbf{J}_1^B = \mathbf{J}_1^G, \quad C_{21}^B = C_2^G, \quad \mathbf{J}_2^B = \mathbf{J}_2^G. \tag{18}$$

Remaining conditions:

$$x \rightarrow \infty: \mathbf{J}_1^j = \mathbf{J}_2^j = 0, \quad y = 0,$$

$$y = \Delta + h_g: \mathbf{J}_1^j = \mathbf{J}_2^j = 0, \quad j = B, G. \tag{19}$$

The conditions (19) are true for both grains and grain boundaries.

2. A method for solving the thermodiffusion problem

Let's use dimensionless variables for the numerical solution of problem (13):

$$\xi = \frac{r}{x_*}, \quad \theta = \frac{T - T_0}{T_* - T_0},$$

$$\tau = \frac{t}{t_*}, \quad \bar{\mathbf{J}}_i = \frac{\mathbf{J}_i}{\mathbf{J}_*}, \quad \bar{\mathbf{J}}_q = \frac{\mathbf{J}_q}{\mathbf{J}_{q*}},$$

where the following scales are used: $x_* R_2$ — the outer radius of the part, $t_* = t_i$ — the duration of the external pulse, $T_* = \frac{q_0 x_*}{\lambda_T} + T_0$, $\mathbf{J}_* = \frac{\rho \kappa_T}{R_2}$, $\mathbf{J}_{q*} = \frac{\lambda_T (T_* - T_0)}{x_*}$, and $\kappa_T = \frac{\lambda_T}{\rho C_\sigma}$ —

Table 2. Notation of the dimensionless problem formulation (20)–(26)

$\bar{\Phi}_1 = C_3 C_1^2 \exp\left(\frac{\varepsilon_1 (\theta-1)}{Ar (\theta+\sigma)}\right)$, $\bar{\Phi}_2 = C_3 C_2^2 \exp\left(\frac{\varepsilon_2 (\theta-1)}{Ar (\theta+\sigma)}\right)$	$L_1 = \frac{D_1^0 C_{\sigma\rho}}{\lambda_T} \exp\left(-\frac{E_{D1}}{RT_*}\right)$
$\Phi_{D1} = \exp\left(\frac{1}{Ar} \frac{(\theta-1)}{(\theta+\sigma)}\right)$, $\Phi_{D2} = \exp\left(\frac{\varepsilon_D (\theta-1)}{Ar (\theta+\sigma)}\right)$	$L_2 = \frac{D_2^0 C_{\sigma\rho}}{\lambda_T} \exp\left(-\frac{E_{D2}}{RT_*}\right)$
$\bar{Q}_1^\sigma = \frac{Q_1^\sigma}{\rho C_\sigma (T_* - T_0)}$, $\bar{Q}_2^\sigma = \frac{Q_2^\sigma}{\rho C_\sigma (T_* - T_0)}$	$\bar{S}_{T1} = S_{T1} (T_* - T_0)$; $\bar{S}_{T2} = S_{T2} (T_* - T_0)$
$\bar{k}_1 = t_* k_1 \exp\left(-\frac{E_1}{RT_*}\right)$, $\bar{k}_2 = t_* k_2 \exp\left(-\frac{E_2}{RT_*}\right)$	$\sigma = \frac{T_0}{T_* - T_0}$, $Ar = \frac{RT_*}{E_{D1}}$, $\delta = \frac{R_1^0}{\kappa t_*}$
$\bar{A}_1 = (\theta + \sigma)^2 [L_1 \gamma_1 \Phi_{D1} f_{11}^0 \bar{S}_{T1} f_{11}^0 + L_2 \gamma_2 \Phi_{D2} f_{21}^0 \bar{S}_{T2} f_{22}^0]$	$\varepsilon_1 = \frac{E_1}{E_{D1}}$; $\varepsilon_2 = \frac{E_2}{E_{D1}}$; $\varepsilon_D = \frac{E_{D2}}{E_{D1}}$
$\bar{A}_2 = (\theta + \sigma)^2 [L_1 \gamma_1 \Phi_{D1} f_{12}^0 \bar{S}_{T1} f_{11}^0 + L_2 \gamma_2 \Phi_{D2} f_{22}^0 \bar{S}_{T2} f_{22}^0]$	$\gamma_1 = \frac{\rho R_1}{m_1 C_\sigma}$; $\gamma_2 = \frac{\rho R_2}{m_2 C_\sigma}$
$f_{11}^0 = 1 + \frac{m_1}{m_3} \frac{C_1}{1 - C_1 - C_2}$, $f_{22}^0 = 1 + \frac{m_2}{m_3} \frac{C_2}{1 - C_1 - C_2}$	$\bar{W} = \bar{Q}_1^\sigma \bar{k}_1 \bar{\varphi}_1 + \bar{Q}_2^\sigma \bar{k}_2 \bar{\varphi}_2$
$f_{12}^0 = 1 - \frac{m_1}{m_3} \frac{C_1}{1 - C_1 - C_2}$, $f_{21}^0 = 1 - \frac{m_2}{m_3} \frac{C_2}{1 - C_1 - C_2}$	$\tau_1 = \frac{t_1}{t_*}$; $\tau_2 = \frac{t_2}{t_*}$; $\tau_q = \frac{t_q}{t_*}$

the thermal conductivity coefficients, dimensionally coinciding with the diffusion coefficients. In this case the problem will have the following form

$$\tau_q \frac{\partial^2 \theta}{\partial \tau^2} + \frac{\partial \theta}{\partial \tau} = \frac{1}{\delta} \frac{1}{\xi} \frac{\partial}{\partial \xi} \left(\xi \cdot \frac{\partial \theta}{\partial \xi} \right) + \frac{1}{\delta} \frac{1}{\xi} \frac{\partial}{\partial \xi} \left(\xi \cdot \bar{A}_1 \frac{\partial C_1}{\partial \xi} \right) + \frac{1}{\delta} \frac{1}{\xi} \frac{\partial}{\partial \xi} \left(\xi \cdot \bar{A}_2 \frac{\partial C_2}{\partial \xi} \right) + \tau_q \frac{\partial \bar{W}}{\partial \tau} + \bar{W}, \quad (20)$$

$$\tau_1 \frac{\partial^2 C_1}{\partial \tau^2} + \frac{\partial C_1}{\partial \tau} = \frac{L_1}{\delta} \frac{1}{\xi} \frac{\partial}{\partial \xi} \left(\xi \cdot f_{11}^0 \Phi_{D1} \frac{\partial C_1}{\partial \xi} \right) + \frac{L_2}{\delta} \frac{1}{\xi} \frac{\partial}{\partial \xi} \left(\xi \cdot f_{12}^0 \Phi_{D1} \frac{\partial C_2}{\partial \xi} \right) + \frac{L_1 \bar{S}_{T1}}{\delta} \frac{1}{\xi} \frac{\partial}{\partial \xi} \left(\xi \cdot C_1 f_{11}^0 \Phi_{D1} \frac{\partial \theta}{\partial \xi} \right) - \tau_1 \frac{\partial \bar{r}_1}{\partial \tau} - \bar{r}_1, \quad (21)$$

$$\tau_2 \frac{\partial^2 C_2}{\partial \tau^2} + \frac{\partial C_2}{\partial \tau} = \frac{L_2}{\delta} \frac{1}{\xi} \frac{\partial}{\partial \xi} \left(\xi \cdot f_{21}^0 \Phi_{D2} \frac{\partial C_1}{\partial \xi} \right) + \frac{L_2}{\delta} \frac{1}{\xi} \frac{\partial}{\partial \xi} \left(\xi \cdot f_{22}^0 \Phi_{D2} \frac{\partial C_2}{\partial \xi} \right) + \frac{L_2 \bar{S}_{T2}}{\delta} \frac{1}{\xi} \frac{\partial}{\partial \xi} \left(\xi \cdot C_2 f_{22}^0 \Phi_{D2} \frac{\partial \theta}{\partial \xi} \right) - \tau_2 \frac{\partial \bar{r}_2}{\partial \tau} - \bar{r}_2, \quad (22)$$

$$\frac{dC_4}{d\tau} = \bar{r}_4, \quad (23)$$

$$\frac{dC_5}{d\tau} = \bar{r}_5, \quad (24)$$

$$\tau = 0: C_i = C_{i0}(\xi), \quad I = 1-5, \quad \theta = 0. \quad (25)$$

$$\xi = 1: \bar{J}_i = 0 \quad i = 1, 2, \quad \bar{J}_q = \begin{cases} 1, & \tau < 1, \\ 0, & \tau \geq 1. \end{cases} \quad (26)$$

Functions, coefficients and parameters are listed in Table 2.

The dimensionless parameters introduced in the dimensionless formulation of the problem have a well-defined physical meaning and represent relations of characteristic scales of different processes. For example, δ — an

equivalent of the Frank-Kamenetsky parameter is a square of the ratio of the radius of the product to the value of the thermal boundary layer formed in the part during the pulse exposure; L_1 and L_2 — Lewis numbers or the ratio of the diffusion constants to the thermal conductivity coefficient; \bar{k}_1 and \bar{k}_2 — the ratio of the pulse duration to the characteristic reaction times at a temperature of T_* achieved when the part is heated by a flux of q_0 during the same time; \bar{Q}_1^σ and \bar{Q}_2^σ — the ratio of transfer heats to the heat reserve in the heated layer when it is heated to T_* , etc. The result is a function of their values.

The source terms in the diffusion and kinetics equations have the following the form:

$$\begin{aligned} \bar{r}_1 &= -\bar{\varphi}_2, & \bar{r}_2 &= -2\bar{\varphi}_2, & \bar{r}_3 &= -\bar{\varphi}_1 - \bar{\varphi}_2, \\ \bar{r}_4 &= \bar{\varphi}_1, & \bar{r}_5 &= \bar{\varphi}_2, & \bar{W} &= \bar{Q}_1^\sigma \bar{\varphi}_1 + \bar{Q}_2^\sigma \bar{\varphi}_2. \end{aligned} \quad (27)$$

3. Method for solving the grain boundary diffusion problem

Let's use the other dimensionless variables to numerically solve the problem (16)–(19) at the micro level [16]:

$$X = \frac{x}{x_*}, \quad Y = \frac{y}{y_*}, \quad \tau = \frac{t}{t_*}, \quad \bar{J}_i = \frac{J_i}{J_*},$$

where the following scales are used: $x_* = y_* = \Delta$ — grain-boundary area half-width, t_* — external pulse duration, $J_* = \frac{\Delta}{t_*}$, $\bar{D}_i^j = \frac{t_*}{\Delta^2} D_i^j$, $i = 1, 2$, $j = B, G$. In this case the problem will have the following form

$$\begin{aligned} \tau_1^B \frac{\partial^2 C_1^B}{\partial \tau^2} + \frac{\partial C_1^B}{\partial \tau} &= \bar{D}_1^B \frac{\partial^2 C_1^B}{\partial X^2} + \bar{D}_1^B \frac{\partial^2 C_1^B}{\partial Y^2} - \bar{r}_1^B - \tau_1^B \frac{\partial \bar{r}_1^B}{\partial \tau}, \\ \tau_1^G \frac{\partial^2 C_1^G}{\partial \tau^2} + \frac{\partial C_1^G}{\partial \tau} &= \bar{D}_1^G \frac{\partial^2 C_1^G}{\partial X^2} + \bar{D}_1^G \frac{\partial^2 C_1^G}{\partial Y^2} - \bar{r}_1^G - \tau_1^G \frac{\partial \bar{r}_1^G}{\partial \tau}, \\ \tau_2^B \frac{\partial^2 C_2^B}{\partial \tau^2} + \frac{\partial C_2^B}{\partial \tau} &= \bar{D}_2^B \frac{\partial^2 C_2^B}{\partial X^2} + \bar{D}_2^B \frac{\partial^2 C_2^B}{\partial Y^2} - \bar{r}_2^B - \tau_2^B \frac{\partial \bar{r}_2^B}{\partial \tau}, \\ \tau_2^G \frac{\partial^2 C_2^G}{\partial \tau^2} + \frac{\partial C_2^G}{\partial \tau} &= \bar{D}_2^G \frac{\partial^2 C_2^G}{\partial X^2} + \bar{D}_2^G \frac{\partial^2 C_2^G}{\partial Y^2} - \bar{r}_2^G - \tau_2^G \frac{\partial \bar{r}_2^G}{\partial \tau}. \end{aligned} \quad (28)$$

Table 3. Physical values of substances and compounds

Value	Hydrogen	Oxygen	Alloy Zr	ZrH ₂	ZrO ₂
E, kJ/mol	34.704–47.239	72.3–120.5	141–172	25.3	12.8
S, kJ/(mol·K)	131	205	39.08	35.2	50.4
H, kJ/mol	39.2	966.5	–1099	–166.1	–1100.6
m, kg/mol	1 · 10 ^{–3}	16 · 10 ^{–3}	91 · 10 ^{–3}	93 · 10 ^{–3}	123 · 10 ^{–3}
ρ, kg/m ³	0.09	1141	6511	5620	6000
λ, W/(m·K)	0.167	0.0258	20.96	–	2.5
C _p , kJ/(kg·K)	14.5	0.919	0.291	–	0.4
T _{melt} , K	13	54	2128	1073	2973

Table 4. Formal kinetic parameters of reactions

Parameters	I	II
k _i , 1/s	1.60 · 10 ²²	3.90 · 10 ²¹
E _{ai} , J/mol	4.48 · 10 ⁴	1.739 · 10 ⁵
Q, J/m ³	–166.1	–1100.6

Conditions at the external boundaries

$$X = 0: \quad C_1^j = C_{10}, \quad C_2^j = C_{20},$$

$$X \rightarrow \infty: \quad C_i^j = 0. \quad (29)$$

$$Y = 0, \quad Y = \bar{h}_g + 1: \quad \bar{\mathbf{J}}_i^B = \bar{\mathbf{J}}_i^G = 0.$$

Conditions at the internal boundaries

$$C_B = C_G, \quad \bar{\mathbf{J}}_i^b = \bar{\mathbf{J}}_i^G. \quad (30)$$

Initial conditions

$$\tau = 0: \quad C_i^B = 0, \quad \frac{\partial C_i^B}{\partial \tau} = \frac{\partial C_i^B}{\partial \tau} = 0, \quad (31)$$

$$i = 1, 2, j = B, G.$$

4. Evaluation of model parameters

It is useful to estimate the range of parameter variation since some of the physical quantities that are known and listed in the table 3 and 4 are either highly inaccurate or poorly defined. We will find the following using the properties of Zr, H, O, ZrH₂, ZrO₂ provided in the literature [17–27]. $Ar = [10^{-2} \dots 0.3]$, $\sigma = [0.5 \dots 1.5]$, $L_1 = [10^{-2} \dots 10^{-1}]$, $L_2 = [10^{-2} \dots 10^{-1}]$, $\bar{S}_{T1} = [10^{-1} \dots 20]$, $\bar{S}_{T2} = [10^{-1} \dots 20]$, $\varepsilon_D = [0.5 \dots 1.5]$, $\tau_1 = [10^{-2} \dots 30]$, $\tau_2 = [10^{-3} \dots 30]$, $\tau_q = [10^{-1} \dots 10]$, $\bar{k}_1 = [10^5 \dots 10^7]$, $\bar{k}_2 = [10^4 \dots 10^6]$, $\bar{Q}_1^6 = [10^{-2} \dots 10]$, $\bar{Q}_2^6 = [10^{-2} \dots 10]$. We see that the parameters of the model vary in a wide range.

5. The problem of mechanical equilibrium

The problem of the mechanical equilibrium of a hollow cylinder is the second part of the problem. It is necessary to find stresses in a hollow cylinder of finite dimensions caused by a short-term thermal pulse. Gravity and external pressure can be ignored. Ignoring the impacts of the ends, it can be assumed that the cylinder cross sections which are perpendicular to the cylinder axis remain flat and work under the same conditions, so that radial movements depend only on the radius. In this case, the problem of equilibrium in a cylindrical coordinate system will be one-dimensional. The following ratios are true for this problem: $\varepsilon_{rr} = \frac{du}{dr}$, $\varepsilon_{\varphi\varphi} = \frac{u}{r}$, $\varepsilon_{r\varphi} = \varepsilon_{rz} = \varepsilon_{\varphi,z} = 0$.

The hypothesis of flat cross sections allows assuming that the relative elongation in the direction of z is a constant value, $\varepsilon_{zz} = \text{const}$.

Then this value is expressly present in all formulas and requires calculation based on an additional condition. The equilibrium equations for the selected conditions have the following form in the cylindrical coordinate system: $\frac{d\sigma_{rr}}{dr} + \frac{\sigma_{rr} - \sigma_{\varphi\varphi}}{r} = 0$.

Boundary condition

$$r = R_0: \quad \sigma = 0 \quad (32)$$

indicates that the internal surface is not stressed. The outer surface is also not stressed:

$$r = R_1: \quad \sigma = 0. \quad (33)$$

The following notations are used in (32), (33): σ — radial component of the stress tensor, u — radial displacement. It is necessary to add the Duhamel–Neumann relation to the above equations and conditions which has the following form for our problem

$$\sigma_{rr} = \frac{(1-\nu)E}{(1-2\nu)(1+\nu)} \frac{du}{dr} + \frac{\nu E}{(1-2\nu)(1+\nu)}$$

$$\times \left(\frac{u}{r} + \varepsilon_{zz} \right) - \frac{E}{3(1-2\nu)} \omega,$$

$$\sigma_{\varphi\varphi} = \frac{(1-\nu)E}{(1-2\nu)(1+\nu)} \frac{u}{r} + \frac{\nu E}{(1-2\nu)(1+\nu)}$$

$$\times \left(\frac{du}{dr} + \varepsilon_{zz} \right) - \frac{E}{3(1-2\nu)} \omega,$$

$$\begin{aligned} \sigma_{zz} &= \frac{(1-\nu)E}{(1-2\nu)(1+\nu)} \varepsilon_{zz} + \frac{\nu E}{(1-2\nu)(1+\nu)} \\ &\times \left(\frac{u}{r} + \frac{du}{dr} \right) - \frac{E}{3(1-2\nu)} \omega, \quad (34) \\ \sigma_{r\varphi} &= \sigma_{rz} = \sigma_{\varphi z} = 0, \end{aligned}$$

where E and ν — modulus of elasticity and Poisson's ratio.

We obtain $\omega = 3 [\alpha_T(T - T_0) + \sum_{i=1}^n \alpha_i(C_i - C_{i0})]$ taking into account thermal stresses and concentration stresses, where α_i — linear coefficients of concentration expansion, α_T — linear coefficient of thermal expansion; C_i — mass concentrations of components (reagents and reaction products), $i = 1, 2, 3, 4, 5$.

The solution to the equilibrium problem has the following form

$$\begin{aligned} u &= \frac{1}{3} \frac{1+\nu}{1-\nu} \frac{1}{r} \int_{P_0}^r \omega(r) r dr + \frac{P}{2} r + \frac{B}{r}, \\ \varepsilon_{rr} \equiv \varepsilon &= \frac{1}{3} \frac{1+\nu}{1-\nu} \left[\omega(r) - \frac{1}{r^2} \int_{R_0}^r \omega(r) r dr \right] + \frac{P}{2} - \frac{B}{r^2}, \\ \varepsilon_{\varphi\varphi} \equiv \varepsilon &= \frac{1}{3} \frac{1+\nu}{1-\nu} \int_{R_0}^r \omega(r) r dr + \frac{P}{2} + \frac{B}{r^2}, \\ \sigma &= -\frac{E}{3(1-\nu)} \frac{1}{r^2} \int_{R_0}^r \omega(r) r dr + \frac{E}{(1-2\nu)(1+\nu)} \\ &\times \left[\frac{P}{2} + \nu \varepsilon_{zz} \right] - \frac{1}{r^2} \frac{BE}{1+\nu}. \end{aligned}$$

Here A, B — integration constants. Next, we will introduce new integration „constants“ for convenience

$$F = \frac{E}{(1-2\nu)(1+\nu)} \left[\frac{A}{2} + \nu \varepsilon_{zz} \right], \quad G = \frac{BE}{1+\nu}. \quad (35)$$

Then the expressions for nonzero components of stress and strain tensors will have the following form

$$\sigma = -\frac{E}{3(1-\nu)} \frac{1}{r^2} \int_{R_0}^r \omega(r) r dr + F - \frac{G}{r^2}, \quad (36)$$

$$\sigma_{\varphi\varphi} = \frac{E}{3(1-\nu)} \int_{R_0}^r \omega(r) r dr + F + \frac{G}{r^2} - \frac{E}{3(1-\nu)} \omega, \quad (37)$$

$$\sigma_{zz} = -\frac{E}{3(1-\nu)} \omega + 2F\nu - E\varepsilon_{zz}, \quad (38)$$

$$\varepsilon_{rr} \equiv \varepsilon = \frac{1}{3} \frac{1+\nu}{1-\nu} \left[\omega(r) - \frac{1}{r^2} \int_{R_0}^r \omega(r) r dr \right] + \frac{A}{2} - \frac{B}{r^2}, \quad (39)$$

$$\varepsilon_{\varphi\varphi} \equiv \varepsilon = \frac{1}{3} \frac{1+\nu}{1-\nu} \frac{1}{r^2} \int_{R_0}^r \omega(r) r dr + \frac{A}{2} - \frac{B}{r^2}. \quad (40)$$

The integration constants and the value are found using conditions (32)–(34).

6. Dimensionless variables in the mechanical equilibrium problem

We use the dimensionless variables in the resulting solution (26)–(30):

$$S = \frac{\sigma}{\sigma_*}, \quad e = \frac{\varepsilon}{\varepsilon_*}, \quad \bar{\omega} = \frac{\omega}{\omega_*},$$

$$\bar{u} = \frac{u}{u_*}, \quad \xi = \frac{r}{x_*},$$

where $S = S_{rr}$ ($S_{\varphi\varphi}$), $e = e_{rr}$ ($e_{\varphi\varphi}, e_{zz}$), and $\sigma_* = 3E\alpha_T(T_* - T_0)$, $\varepsilon_* = 3\alpha_T(T_* - T_0)$, $\omega_* = 3\alpha_T(T_* - T_0)$, $u_* = \omega_* x_*$ — scales consistent with the previous one.

Equations (36)–(40) in dimensionless variables and boundary conditions will have the following form

$$S_{rr} = -\frac{1}{3(1-\nu)} \frac{1}{\xi^2} \int_{\xi_0}^{\xi} \bar{\omega}(\xi) \xi d\xi + \bar{F} - \frac{\bar{G}}{\xi^2}, \quad (41)$$

$$S_{\varphi\varphi} = \frac{1}{3(1-\nu)} \int_{\xi_0}^{\xi} \bar{\omega}(\xi) \xi d\xi + \bar{F} + \frac{\bar{G}}{\xi^2} - \frac{1}{3(1-\nu)} \bar{\omega}, \quad (42)$$

$$S_{zz} = -\frac{1}{3(1-\nu)} \bar{\omega} + 2\bar{F}\nu - e_{zz}, \quad (43)$$

$$e_{rr} = \frac{1}{3} \frac{1+\nu}{1-\nu} \left[\bar{\omega}(\xi) - \frac{1}{\xi^2} \int_{\xi_0}^{\xi} \bar{\omega}(\xi) \xi d\xi \right] + \frac{\bar{P}}{2} - \frac{\bar{B}}{\xi^2}, \quad (44)$$

$$e_{\varphi\varphi} = \frac{1}{3} \frac{1+\nu}{1-\nu} \frac{1}{\xi^2} \int_{\xi_0}^{\xi} \bar{\omega}(\xi) \xi d\xi + \frac{\bar{P}}{2} - \frac{\bar{B}}{\xi^2}, \quad (45)$$

$$\xi = \xi_0: \quad S = 0, \quad (46)$$

$$\xi = 1: \quad S = 0, \quad (47)$$

where

$$\bar{\omega} = \theta + \sum_{k=1}^n g_k (C_k - C_{k0}), \quad g_k = \frac{\alpha_k - \alpha_{k0}}{\alpha_T(T_* - T_0)},$$

$$k = 1-5, \quad \bar{F} = \frac{F}{3E\alpha_T(T_* - T_0)}, \quad \bar{G} = \frac{G}{3E\alpha_T(T_* - T_0)},$$

$$\bar{P} = \frac{P}{3\alpha_T(T_* - T_0)}, \quad \bar{B} = \frac{B}{3\alpha_T(T_* - T_0)}.$$

A system of linear algebraic equations with respect to the integration constants will be obtained by substituting (41)–(45) in conditions (46),(47). The system of equations in new notation for finding constants \bar{F}, \bar{G} is based on the written boundary conditions:

$$\bar{F} - \frac{\bar{G}}{\xi_0^2} = 0, \quad (48)$$

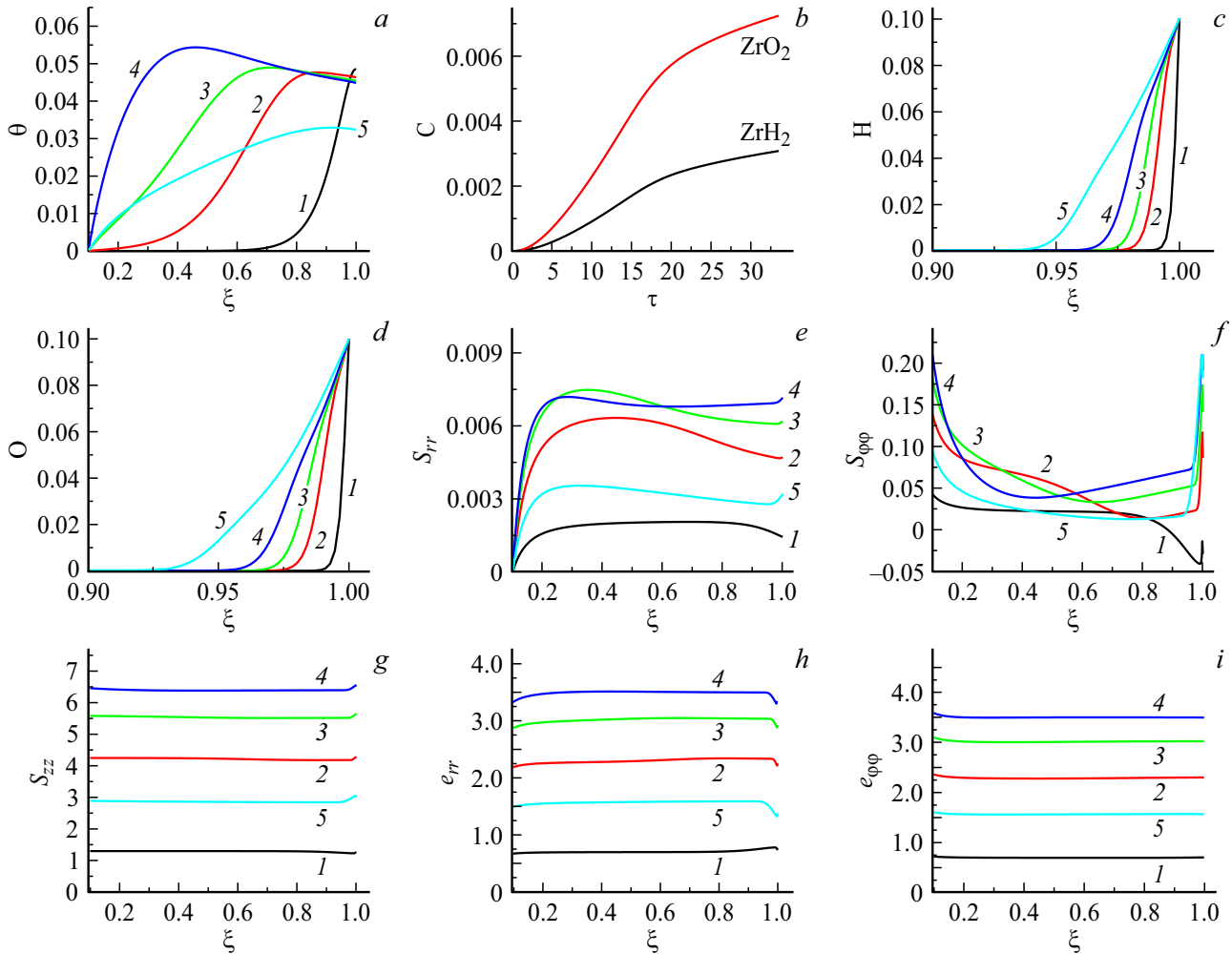


Figure 2. Distribution of temperature(a), hydrogen and oxygen concentrations (c, d), stresses (e–g), deformations (h, i) over space at successive time points, τ : 1 – 1, 2 – 4, 3 – 6, 4 – 9, 5 – 15 and concentrations of substances produced by reactions over time (b) taking into account chemical reactions $k_1 = 1 \cdot 10^4$, $k_2 = 3 \cdot 10^5$.

$$-\frac{1}{3} \frac{1+\nu}{1-\nu} \frac{1}{\xi_1} \int_{\xi_0}^{\xi_1} \bar{\omega}(\xi) \xi d\xi + \bar{F} - \frac{\bar{G}}{\xi_1^2} = 0, \quad (49)$$

$$2\bar{F}_v = e_{zz}. \quad (50)$$

The system (48)–(50) allows finding \bar{F} , \bar{G} and e_{zz} , which have the following form

$$\bar{F} = \frac{\xi_1}{\xi_1^2 - \xi_0^2} \frac{1+\nu}{3} \frac{1}{1-\nu} \int_{\xi_0}^{\xi_1} \bar{\omega}(\xi) \xi d\xi,$$

$$\bar{G} = \frac{\xi_0^2 \xi_1}{\xi_1^2 - \xi_0^2} \frac{1+\nu}{3} \frac{1}{1-\nu} \int_{\xi_0}^{\xi_1} \bar{\omega}(\xi) \xi d\xi,$$

$$e_{zz} = \frac{2\nu \xi_1}{\xi_1^2 - \xi_0^2} \frac{1+\nu}{3} \frac{1}{1-\nu} \int_{\xi_0}^{\xi_1} \bar{\omega}(\xi) \xi d\xi.$$

Problem (14)–(20) was solved numerically using a specially developed algorithm based on an implicit second-order difference scheme in space and time for the differential equation of thermal conductivity and diffusion. The nonlinear multipliers and terms on each time layer were linearized and calculated using quantities which were already known from the previous layer. The obtained difference equations were reduced to a form that was convenient for the application of the elimination method. The boundary conditions are also approximated using the second order of approximation by decomposition of grid functions at points closest to the boundary into Taylor series relative to the boundary points. The convergence was verified by extrapolation to the zero step. The implementation of the law of conservation of mass was monitored in all calculations.

The components of stress and strain tensors were calculated using formulas (41)–(45) and Table 4. The following parameters were used: $Ar = 0.3$, $\sigma = 0.6$, $L_1 = 1 \cdot 10^{-1}$;

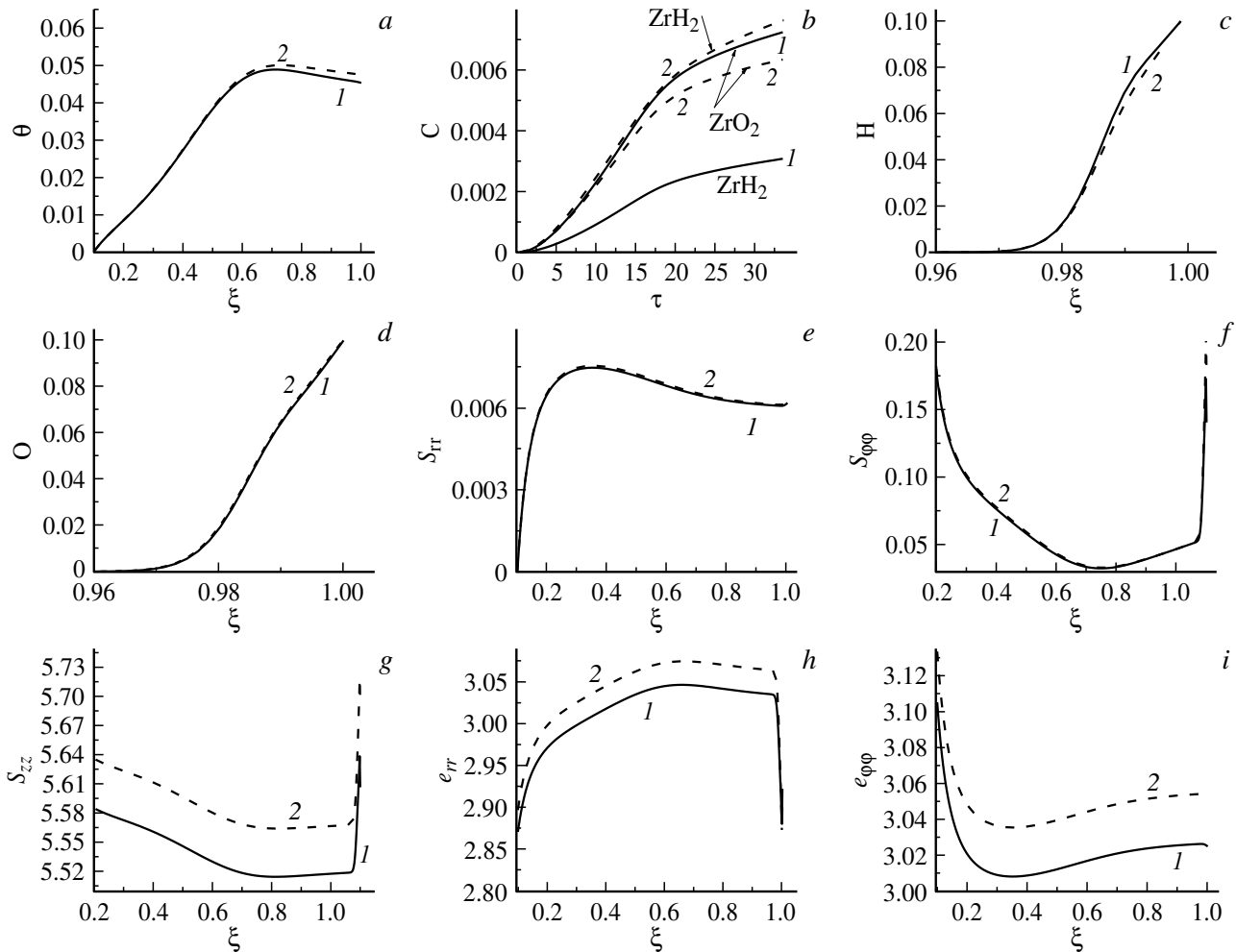


Figure 3. Distribution of temperature (a), concentrations of hydrogen and oxygen (c,d), stresses (e–g), strains (h,i) in space at successive time points $\tau = 6$ and concentrations of substances produced by reactions in time (b), with varying velocity constants of the first reaction: 1 — $k_1 = 1 \cdot 10^4$, $k_2 = 3 \cdot 10^5$; 2 — $k_1 = 4 \cdot 10^4$, $k_2 = 3 \cdot 10^5$.

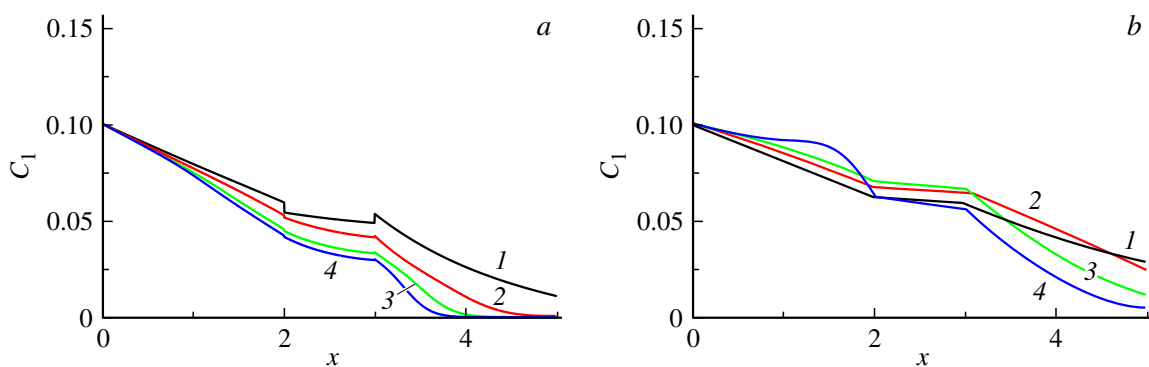


Figure 4. Concentrations of diffusing hydrogen in the grain-boundary region ($Y = 0.5$) (a) and in the intragrain regions ($Y = 1.5$) (b) with different relaxation times. Grain size $\bar{h}_g = 2$, ratio of diffusion constants $\bar{D}_B/\bar{D}_G = 10$, reaction velocity ratio $k_B/k_G = 200$. Half of the width of the grain boundary area is assumed as a unit length scale. The distributions are shown at time point $\tau = 27$. 1 — $\tau_B = \tau_G = 0$; 2 — $\tau_B = 5$, $\tau_G = 10$; 3 — $\tau_B = 10$, $\tau_G = 20$; 4 — $\tau_B = 15$, $\tau_G = 30$.

$L_2 = 3 \cdot 10^{-1}$; $\delta = 50$, $\varepsilon_D = 1$, $\varepsilon_1 = 2.1$, $\varepsilon_2 = 2.6$, $\gamma_1 = 1$, $\gamma_2 = 1$, $\bar{Q}_1^\sigma = 5$, $\bar{Q}_2^\sigma = 3$, $g_1 = 0.6$, $g_2 = 0.9$, $g_3 = 1.8$, $g_4 = 1.2$, $g_5 = 1.4$, $\bar{\alpha}_T = 1.2$, $\xi_0 = 0.1$, $\xi_1 = 1$, $\bar{E} = 1$,

$\tau_1 = 5$, $\tau_2 = 5$, $\tau_q = 10$. The following varying dimensionless parameters were used in the calculations: \bar{k}_1 , \bar{k}_2 — reaction rate constants, \bar{S}_{T1} , \bar{S}_{T2} — Soret coefficients.

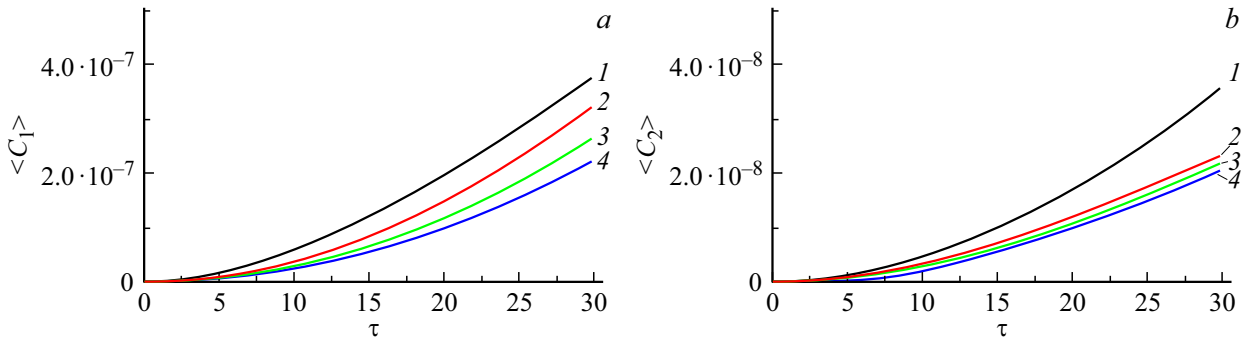


Figure 5. Average concentrations of reaction products in case of different relaxation times at different time points. Grain size $\bar{h}_g = 2$, ratio of diffusion constants $\bar{D}_B/\bar{D}_G = 10$, reaction velocity ratio $k_B/d_G = 200$. Half of the width of the grain boundary area is assumed as a unit length scale. 1 — $\tau_B = \tau_G = 0$; 2 — $\tau_B = 5$, $\tau_G = 10$; 3 — $\tau_G = 10$, $\tau_G = 20$; 4 — $\tau_B = 15$, $\tau_G = 30$.

7. Analysis of numerical results

The distribution of temperature, concentrations, stresses and strains at successive time points at relaxation times $\tau_1 = 5$, $\tau_2 = 5$, $\tau_3 = 10$ is shown on Fig. 2. A heat wave moves from the outer surface of the part with the selected set of parameters (Fig. 2, *a*). Hydrogen and oxygen (Fig. 3, *c, d*) diffuse deeper into the substrate and, as a result of reactions, zirconium oxide and zirconium hydride are formed near the outer surface of the sample (Fig. 2, *b*). Fig. 2, *b* shows average integral concentrations of zirconium oxide and zirconium hydride. Stresses and strains increase (Fig. 2, *e–h*, lines 1–3), and begin to decrease (Fig. 2, *e–h*, the lines 4, 5) from the time point greater than the maximum relaxation time ($\tau_q = 10$). Distortions can be seen near the outer boundary on the tangential stress wave (Fig. 2, *f*), which correspond to the composition varying over time (formation of zirconium oxide and zirconium hydride).

The zirconium hydride concentration increases with an increase of the rate constant of the first reaction, i.e. the formation of zirconium hydride (Fig. 3), and the concentration of hydrogen and zirconium oxide decreases while the temperature increases slightly. Radial stresses and strains increase, which is obviously clearly related to changes of composition.

An increase of the rate constant of the second reaction (formation of zirconium oxide) has virtually no impact on the distribution of concentration, radial and tangential stresses and only slightly affects the temperature distribution in the sample, which is associated with an increase of the heat release in the result of the reaction (not shown in the figure). The accounting for the Soret and Dufour effects is more evident in the distribution of stresses and strains (not shown in the picture). The qualitative nature of the distributions of all quantities does not change.

Some examples of calculations of processes taking place at the micro level are provided below. Higher concentrations of the diffusant will be observed in the intragrain region, where its accumulation takes place. Concentration waves in grain boundary regions are clearly visible in case of short times slightly exceeding the relaxation times (Fig. 4). That

said, the longer the relaxation time, the more clearly these waves are expressed.

The formation of reaction products can be described in terms of average concentrations of $\langle C_i \rangle = \frac{1}{S} \int_{\Omega_s} C_i ds$, $i = 1, 2$, S — area of the region of interest Ω_s (Fig. 5).

Therefore, products are formed more slowly in average with higher relaxation times.

Conclusion

The study presents a macromodel of the evolution of the composition of a cylindrical sample under conditions of short-term thermal exposure. The impact of the Soret and Dufour effects and the rate constants of the two reactions on temperature and concomitant stresses is illustrated in the paper. The diffusants accumulate in the intragrain region at the microlevel, taking into account the grain structure of the material, and diffusants are rapidly consumed in the grain-boundary region. The nature of the stress and strain distribution is affected by the Soret and Dufour effects and changes in composition, including the effect of the rate constants of the zirconium oxide and zirconium hydride formation reactions. The saturation of the material surface areas with diffusers has a wave-like character when mass flux relaxation phenomenon is taken into account. The obtained results and a similar approach to solving the problem can be applied to describe the operation of metal products under extreme conditions.

Acknowledgments

The authors consider it their pleasant duty to express gratitude to A.G. Knyazeva for her help in formulating the problem and useful discussions.

Funding

This study was supported financially by grant from the Russian Foundation for Basic Research and ROSATOM State Corporation No.20-21-00064.

Conflict of interest

The authors declare that they have no conflict of interest.

References

- [1] R.W. Cahn, P. Haasen, E.J. Kramer. *Materials Science and Technology* (WILEY-VCH Verlag GmbH & Co KGaA, NY., 1994)
- [2] S.A. Nikulin. *Tsirkonievye splavy dlya yadernykh energeticheskikh reaktorov* (Izd-vo „MISIS“, M., 2007) (in Russian).
- [3] S.J. Zinkle, G.S. Was. *Acta Mater.*, **61** (3), 735 (2013). DOI: 10.1016/j.actamat.2012.11.004
- [4] S.J. Zinkle, L.L. Snead. *Annu. Rev. Mater. Res.*, **44** (1), 241 (2014). DOI: 10.1146/annurev-matsci-070813-113627
- [5] T. Allen, J. Busby, M. Meyer, D. Petti. *Mater. Today*, **13** (12), 14 (2010). DOI: 10.1016/S1369-7021(10)70220-0
- [6] B. Ensor, A.M. Lucente, M.J. Frederick, J. Sutliff, A.T. Motta. *J. Nucl. Mater.*, **496**, 301 (2017). DOI: 10.1016/j.jnucmat.2017.08.046
- [7] Z. Duan, H. Yang, Y. Satoh, K. Murakami, S. Kano, Z. Zhao, J. Shen, H. Abe. *Nucl. Eng. Design*, **316**, 131 (2017). DOI: 10.1016/j.nucengdes.2017.02.031
- [8] C. Herzig, S.V. Divinski. *Mater. Transactions*, **44** (1), 14 (2003).
- [9] C. Suryanarayana, C.C. Koch. *Hyperfine Interactions*, **130** (5), 5 (2000).
- [10] L. Chen, Z. Wang, H. Zhu, P.A. Burr, J. Qu, Yi. Huang, L. Balogh, M. Preuss, O. Muránsky. *Scripta Mater.*, **210**, 114410 (2022). DOI: 10.1016/j.scriptamat.2021.114410
- [11] I.P. Chernov, S.V. Ivanova, M.H. Krening, N.V. Koval, V.V. Larionov, A.M. Leader, N.S. Pushilina, E.N. Stepanova, O.M. Stepanova, Y.P. Cherdantsev. *ZhTF*, **82** (3), 81 (2012) (in Russian).
- [12] I.P. Chernov, N.S. Pushilina, E.V. Berezneeva, A.M. Leader, S.V. Ivanova. *ZhTF*, **83** (9), 38 (2013) (in Russian).
- [13] I.P. Chernov, E.V. Berezneeva, P.A. Beloglazova, S.V. Ivanova, I.V. Kireeva, A.M. Leader, G.E. Remnev, N.S. Pushilina, Y.P. Cherdantsev. *ZhTF*, **84** (4), 68 (2014) (in Russian).
- [14] I.P. Chernov, E.V. Berezneeva, N.S. Pushilina, V.N. Kudiyarov, N.N. Koval, O.V. Krysina, V.V. Shugurov, S.V. Ivanov, A.N. Nikolaeva. *ZhTF*, **85** (2), 102 (2015) (in Russian).
- [15] A.G. Knyazeva, V.G. Demidov. *Vestnik Permskogo gos. tekhn. ta. Mekhanika*, **3**, 84 (2011) (in Russian).
- [16] M.V. Chepak-Giesbrecht, A.G. Knyazev. *Vychislitel'naya mekhanika sploshnykh sred*, **12** (1), 57 (2019) (in Russian).
- [17] A.P. Babichev, N.A. Babushkina, A.M. Bratkovsky, M.E. Brodov, M.V. Bystrov, B.V. Vinogradov, L.I. Vinokurova, E.B. Gelman, A.P. Geppé, I.S. Grigoryev, K.G. Gurtovoy, V.S. Egorov, A.V. Eletsy, L.K. Zarembo, V.Y. Ivanov, V.L. Ivashintseva, V.V. Ignatiev, R.M. Imamov, A.V. Inyushkin, N.V. Kadobnova, I.I. Karasik, K.A. Kikoin, V.A. Krivoruchko, V.M. Kulakov, S.D. Lazarev, T.M. Lifshits, Yu.E. Lubarsky, S.V. Marin, I.A. Maslov, E.Z. Meilikhov, A.I. Migachev, S.A. Mironov, A.L. Musatov, Yu.P. Nikitin, L.A. Novitsky, A.I. Obukhov, V.I. Ozhogin, R.V. Pisarev, Yu.V. Pisarevsky, V.S. Ptuskin, A.A. Radzig, V.P. Rudakov, B.D. Summ, R.A. Sunyaev, M.N. Khlopkin, I.N. Khlustikov, V.M. Cherepanov, A.G. Chertov, V.G. Shapiro, V.M. Shustriakov, S.S. Yakimov, V.P. Yanovsky. *Fizicheskie velichiny*. Spravochnik. Ed. by I.S. Grigor'ev, E.Z. Meilikhov (Energoatomizdat, M., 1991) (in Russian).
- [18] A. Züttel. *Materials for Hydrogen Storage*, **6** (9), 24 (2003).
- [19] A. Züttel, A. Borgschulte, L. Schlapbach. *Hydrogen as a Future Energy Carrier* (WILEY-VCH Verlag GmbH & Co. KGaA, Weinheim, 2008)
- [20] T.P. Chernyaeva, A.V. Ostapov. *Voprosy atomnoy nauki i tekhniki*, **2**, 3 (2014) (in Russian).
- [21] R.K. Siripurapu. *Intern. J. Nucl. Energy*, **2014**, 1 (2014).
- [22] K. McKay. *Vodorodnye soedineniya metallov* (Mir, M., 1968) (in Russian).
- [23] C. Juillet, M. Tupin, F. Martin, Q. Auzoux, C. Berthier, F. Miserque, F. Gaudier. *Intern. J. Hydrogen Energy*, **44** (39), 21264 (2019). <https://doi.org/10.1016/j.ijhydene.2019.06.034>
- [24] X. Ma, C. Toffolon-Masclet, T. Guilbert, D. Hamon, J.C. Brachet. *J. Nucl. Mater.*, **377**, 359 (2008). <https://doi.org/10.1016/j.jnucmat.2008.03.012>
- [25] M. Arimondi, U. Anselmi-Tamburini, A. Gobetti, Z.A. Munir, G. Spinolo. *J. Phys. Chem. B.*, **101** (41), 8059 (1997).
- [26] A.I. Volkov, I.M. Zharskii, *Bol'shoi khimicheskii spravochnik* (Sovremennaya Shkola, Minsk, 2005) (in Russian).
- [27] P.L. Brown, E. Curty, B. Grambow. *Chemical Thermodynamics of Zirconium* (Elsevier Science, Churchill, 2005)

Translated by A.Akhtyamov